

1 Life history parameters in acellular
2 extrinsic fiber cementum microstructure
3
4

5 Marija Edinborough^{1*}¶, Sarah Fearn^{3&}, Matthew Pilgrim^{4, 5} &, Andrijana Cvetković⁶, Branko
6 Mihailović⁶, Rade Grbić⁶, Kevan Edinborough^{1,7}¶

7
8
9
10 ¹ Melbourne Dental School, Melbourne Dental School, The University of Melbourne,
11 Melbourne, Victoria, Australia

12 ³ Royal School of Mines, Department of Materials, Imperial College London, London, United
13 Kingdom

14 ⁴ Eastman Dental Institute, University College London, London, United Kingdom

15 ⁵ Institute of Ophthalmology, University College London, London, United Kingdom

16 ⁶ Faculty of Medicine, University of Priština, Kosovska Mitrovica, Serbia

17 ⁷ Department of Anthropology, University of British Columbia, Vancouver, Canada

18
19
20 *Corresponding author

21 E-mail: marija.edinborough@unimelb.edu.au
22
23

24 ¶These authors contributed equally to this work.

25 &These authors also contributed equally to this work.
26

27 **Abstract**

28 Life-history parameters such as pregnancies, skeletal trauma, and renal disease have previously
29 been identified from hypomineralized growth layers (incremental lines) of acellular extrinsic
30 fiber cementum (AEFC). The precise periodicity of these growth layers remains vaguely
31 approximated, so causal life-history explanations using tooth cementum cannot yet be
32 rigorously calculated or tested. On the other hand, we show how life history parameters in
33 AEFC can be identified by two contrasting elemental detection methods. Based on our results
34 we reject the possibility of accurate estimation of pregnancies and other life history parameters
35 from cementum using scanning electron microscopy alone. Here, we propose a new
36 methodological approach for cementum research, Time-of-Flight Secondary Ion Mass
37 Spectrometry (ToF-SIMS), to measure degree and distribution of mineralization of cementum
38 growth layers. Our results show that ToF-SIMS can significantly increase our knowledge of
39 cementum composition and is therefore a powerful new tool for life history researchers.

40

41 **Introduction**

42 Acellular extrinsic fiber cementum (AEFC) is deposited in a regular annual rhythm in the form
43 of incremental lines around the roots of human teeth, with varying degrees of mineralization
44 [1, 2]. Life-history parameters (LHP), such as pregnancies, skeletal trauma, and renal disease,
45 can be identified and precisely datable from incremental lines of AEFC in human teeth by
46 observing their visual effects [3]. These life history parameters appear to change calcium
47 metabolism [4, 5], and lack of available calcium at the mineralization front of the cementum
48 causes formation of a such visually different incremental AEFC line [3]. In a study on humans
49 [3], as well as in great apes [6] “suspicious” AEFC lines were successfully detected as being

50 visibly broader and translucent in tooth ground sections (70 - 80 μ m thick) under optical
51 magnification with transmuted polarized light. These studies also showed that some of the
52 LHPs affecting mineralization of AEFC are precisely datable from the AEFC cross-sections.
53 On the other hand, in a controlled study undertaken on goats, Lieberman [2] showed that AEFC
54 bands corresponding to a control diet low in minerals including calcium and phosphorus
55 appeared to be opaquer and relatively narrower, as observed from x-ray microradiographs of
56 thin ground sections (50 μ m thick). Lieberman described these bands as hypermineralized
57 (denser) due to reduced cementogenesis. In contrast, a study undertaken by Cool and
58 colleagues [7] reported that cementum growth layers are not the result of changes in mineral
59 density at all, as they failed to detect cementum growth layers using scanning electron
60 microscope (SEM) equipped with backscattered electrons detector (BSE). The most recent
61 study on composition and structure of AEFC, using Raman imaging analysis [8] argues that
62 darker AEFC lines correspond to higher mineral/organic ratio when compared to brighter lines.

63 However, due to the relatively regular annual rhythm in their layering, AEFC incremental lines
64 are more frequently used as a chronological age estimation aid. This optical detection technique
65 has been in relatively frequent use as an individual age estimation aid [9 - 21], although many
66 results are carefully qualified or subsequently disputed [22, 23]. Continued caution is required,
67 as cementum is the least known of all the mineralized tissues [1], and rigorously controlled
68 human clinical studies have rarely been used to support these findings. As such, life history
69 researchers cannot entirely rely on the results of these pioneering studies yet. Furthermore,
70 cementum research is considerably hampered by an over-emphasis on optical microscopy as
71 summarised by Nadji and colleagues [24]. We do not fully understand the optical appearance
72 of cementum incremental lines yet, let alone the underlying complex mineralisation
73 process(es).

74 Here we investigate if chemical composition and the degree of mineralization of AEFC can
75 detect one important LHP, namely full-term pregnancies, from human teeth. To do so, we
76 employ a comparative approach towards the study of AEFC incremental lines. Firstly, we
77 compared direct measurements of degree and distribution of mineralization of AEFC from a
78 patient with a known life history of six full term pregnancies, using two different microscopic
79 methods, Scanning Electron Microscopy (SEM) with energy Dispersive X-Ray Analysis
80 (EDS) and Time-of-Flight Secondary Ion Mass Spectroscopy (ToF-SIMS).

81

82 **Material and methods**

83 A mandibular canine was extracted from a white Caucasian woman undergoing necessary
84 dental intervention at the University Hospital Kosovska Mitrovica (University of Priština). The
85 informed consent to use the tooth for this research was obtained from the patient as well as her
86 anamnestic data (Table 1). The patient was born and raised in the region of Kosovska
87 Mitrovica. At the time of the extraction she was 66 years old with no previous history of renal
88 disease, endocrinal problems, skeletal fractures or trauma. The patient was considered an
89 excellent candidate for a fertility related analysis, as she reported six pregnancies that carried
90 to full-term, starting at the age of 19 with the last one at age of 31 (Table 1). After the extraction,
91 the tooth was placed in a labelled vial containing physiological saline (solution of 0.90% w/v
92 of NaCl). The tooth was free from obvious signs of pathology.

93

94 **Table 1. The patient's anamnestic data**

Tooth extracted: 43 (left mandibular canine)

Sex: Female

Age of extraction: 66 years

Tooth eruption age: 9.6 years

Age at	19	21	25	27	30	31
--------	----	----	----	----	----	----

pregnancies:

95

96

97 **Scanning Electron Microscopy (SEM) with Energy Dispersive X-**

98 **Ray Analysis (EDS) for measurement of elements**

99 The resin block with exposed mid-root surface represented the sample to be analysed by SEM-
100 EDS was coated with carbon (Quorum K975x carbon coater; Quorum Technologies, UK). The
101 prepared sample was examined at 20 keV by scanning electron microscopy using a Philips
102 XL30 E-SEM (Hillsboro, OR, USA) equipped with an Oxford instruments energy dispersive
103 x-ray analysis detector using Oxford Instruments INCA software. The EDS analysis was
104 employed to determine whether there are mineral component compositional changes between
105 cementum growth layers. EDS analysis was performed on the same sections employed for
106 SIMS imaging. Beam positioning was achieved by viewing the BSE image at 500×
107 magnification.

108 Line scans of cementum growth layers was subject to an acquisition time of 100 sec (working
109 distance 10 mm, take-off angle 35°) to obtain X-ray spectra. The X-ray spectra were used to
110 determine which minerals were present and the Ca:P atomic percent ratio.

111

112 **Identification of Ca and HAp by Time of Flight–Secondary Ion** 113 **Mass Spectrometry Imaging**

114 The sample preparation for ToF-SIMS imaging comprised several steps and it was performed
115 at University College London, Institute of Archaeology. The procedure was tailor made for this
116 research, namely the identification of Ca and HAp from AEFC growth layers using ToF-SIMS.
117 After the cross section was cut out from the mid-root of the patient's tooth, the exposed root
118 surface mounted in the resin represented the sample to be analysed using ToF-SIMS. The
119 following preparation step was polishing, undertaken using a rotating wheel and polishing
120 media. This step is required to remove the surface damage that occurred during sectioning and
121 to provide a flat surface. The polishing procedure included the use of a series of progressively
122 finer polishing pads and diamond compounds, from 2 – ¼ µ (Kemet Diamond paste). The final
123 step was ultrasonic cleaning (1min at xx kHz) using deionized water. This step was performed
124 in order to thoroughly remove all traces of contamination tightly adhering or embedded onto
125 the sample surface.

126 Secondary ion mass spectrometry and secondary ion mapping was performed using a
127 TOF.SIMS5 mass spectrometer (ION-TOF, Münster, Germany) at Imperial College London,
128 Micrometre resolution was used for secondary ion mapping within m/z 0-880. The system is
129 comprised of a bismuth primary ion beam, operating at 25 keV and tuned to use the Bi₃⁺ cluster
130 for greater secondary ion yield, and a low energy electron flood gun for charge compensation.
131 Cluster ion sources, such as Bi₃, are used to identify larger HAp fragment ions at for example
132 m/z 485, 541, 597, and 653, identified as Ca₅P₃O₁₂⁺, Ca₆P₃O₁₃⁺, Ca₇P₃O₁₄⁺, and Ca₈P₃O₁₅⁺,
133 respectively. Ionic species sputtered from the surface under the bismuth bombardment are
134 steered into a reflectron time-of-flight mass analyzer. Before mass spectrometry was
135 performed, an Ar_n⁺ cluster ion beam was used to remove any surface organic contaminants.

136 Identified peaks strongly localized to cementum growth layers were mapped on single ion
137 maps. Positive-ion spectra were acquired from two different 100×100 μm regions of tooth
138 encompassing the entire cementum width from mesio-buccal and disto-buccal side of the tooth,
139 respectively to localize of HAp and identification of different CaP phases within cementum
140 layers.

141 **Study Approval**

142 Use of human tissues and human sensitive data for this study was approved by the Ethics
143 Committee of Faculty of Medicine, University of Pristina at Kosovska Mitrovica, Ministry of
144 Health, Republic of Serbia, as well as by the Ethical Board of Research Executive Agency,
145 European Commission, Brussels.

146 **Results**

147 **SEM-EDS**

148 No visual evidence of cementum growth layering was found SEM micrograph using Philips
149 XL30 FEG-SEM (Hillsboro, OR, USA) equipped with an Oxford instruments energy
150 dispersive x-ray analysis detector (Fig 1a). The Ca:P ratio (by atomic percent) ranged from
151 1.47 to 1.73, with 1.59 as average value. Line scan for Ca showed no significant change in its
152 relative amounts across the width of the cementum (Fig 1b), except in the case of line spectrum
153 (8) which exhibits the lowest relative amount of Ca as of 0.13(atomic %), as well as the lowest
154 Ca:Pa ratio as of 1.29 by atomic % (Fig.1a). However, these low readings for the line spectrum
155 (8) are due to an intruding artefact deposited in cementum, which can be clearly observed on
156 electron photomicrograph of a transverse section of midroot cementum (Fig 1a), and should
157 not be taken into account when interpreting mineral distribution across the AEFC width of our
158 sample.

159

160 **Fig 1. Results of EDS line analysis of the cross section of the patient's tooth.** The SEM
161 photomicrograph of the cross section (a) is showing the location across mid-root acellular
162 extrinsic fiber cementum (AEFC) and dentine (D) where the line spectrum was taken. The line
163 charts (b) represent results of EDS line scan analyses for Ca (upper chart) and Ca/P ratio (lower
164 chart) across the width of AEFC.

165

166 **ToF-SIMS**

167 Layering of AEFC is somewhat visible from the ION-TOF.SIMS5 camera view (Fig 2a), but
168 not in a form of clearly defined incremental lines. Furthermore, AEFC incremental lines in our
169 sample were not clearly discernible even when observed under transmitted polarized light
170 microscope, using 400× magnification, and following the established Tooth Cementum
171 Annulation protocol [25] (see S1 Appendix and S1 Fig). However, we were able to estimate
172 approximal width of AEFC incremental lines in our sample by using the available
173 measurements, and knowledge on teeth eruption AEFC annulation. Having the total width of
174 the intact cementum layer measured from the ToF-SIMS micrograph (Fig 2a) of our sample,
175 assuming that it grows in a regular annual rhythm [1 - 3], we were able to calculate the
176 approximate width of incremental lines. As shown on Figure 2a, the analysed AEFC is flanked
177 by cemento-dentinal junction on one side and outer edge of the tooth on the other side. More
178 precisely, the total width of AEFC in our sample equals 73µm, as it spreads across the area
179 between 4 µm - 77 µm on the linescans (Fig 2b). Given the age of extraction for this tooth (66
180 years), as well as the average sex specific year of eruption of the tooth, which is 9.6 for
181 mandibular canines in females [26, 27], the estimated approximal width of AEFC incremental
182 lines for this individual is c. 1.3 µm.

183 Elemental and molecular maps, as well as line scans of Ca⁺ and HAp⁺ (Ca/P ratio) are obtained
184 from the AEFC surface. We have detected a variation in the intensity of Ca⁺ across the
185 analyzed AEFC surface (Fig 2b). A depletion in relative Ca⁺ intensity can be observed from
186 12 – 54µm respectively, but no depletion in intensity of HAp⁺ in the same line scan (Fig 2b,
187 Fig 3). This corresponds to the patient's 2nd -5th decade of life (Fig 3). The lowest point in Ca⁺
188 intensity depletion is recorded at 32nd µm (Fig 3) which corresponds to start of the patient's 4th
189 decade of life (around age her age of 30).

190

191 **Fig 2. Distribution of the molecular ions identified by SIMS.** (a) A ToF-SIMS micrograph
192 of the area of interest. “D” represents dentine; “AEFC” represents acellular extrinsic fiber
193 cementum; and red square is demarking the area which has been analysed by ToF-SIMS. (b)
194 Molecular ion mapping and line scan ion images of calcium (Ca⁺), and (c) hydroxyapatite
195 (HAp⁺).

196

197 **Fig. 3. Secondary ion yield (counts) of calcium (Ca⁺) and hydroxyapatite (HAp⁺) across**
198 **the width of the cementum.** Right side of the plots represents outside of the tooth.

199

200 **Discussion and conclusions**

201 This study compared two different elemental analyses methods in order to establish which one
202 best estimates the degree and distribution of mineralisation of AEFC. The results of the two
203 methods were compared with the recorded life history parameters of a subject who had six full-
204 term pregnancies. We demonstrate that degree and distribution of mineralization of human

205 AEFC varies across the width of the resultant cementum sample. Furthermore, we show how
206 life history parameter detection in AEFC can vary between two elemental detection methods.
207 Scanning electron microscope with electro-dispersive probe did not detect any significant
208 variation in Ca relative amounts across the AEFC width, nor in Ca:P ratio respectively (Fig
209 1b). The range for the Ca/P ratio (by atomic percent) varied between 1.47 to 1.73, where the
210 majority of the values (Fig 1b) fell below 1.65, and the value 1.73 was read only once. This
211 implies that our results for Ca/P atomic percent ratio are significantly lower than the Ca/P
212 atomic ratio bioapatite standard (1.69 – 1.71). These results suggest that the AEFC analysed
213 here is relatively hypomineralized overall. The aim of this study was to detect variation in
214 degree and distribution of mineralization across the AEFC cross-section, therefore, it is not of
215 any use to discuss the average Ca/P ratio we have obtained. In terms of previous research that
216 found no obvious variation in the concentration profile for calcium and phosphorus, our results
217 are in general agreement [7]. The authors of that study reported that calcium and phosphorus
218 are present in cementum at a ratio (1.70) similar to the bioapatite standard, which disagrees
219 with our results. They concluded that “cementum growth involves a constant rate of both
220 mineralization and matrix production, rather than variations in the rate of matrix production
221 with mineralization continuing at a uniform rate” [7], which is opposite of what was reported
222 in Lieberamn’s work [28] (Lieberman, 1994). Apart from stating that the cross-section was
223 taken through areas shown to contain growth layers, the authors [7] had not specified precisely
224 which type of cementum analyzed in their study. This implies that they were observing
225 cementum as a single uniform type of tissue. A similar approach was taken in a few previous
226 studies when analyzing cementum with electron probes [29, 30]. Importantly, there are various
227 types of cementum which can be distinctly classified based on presence or absence of cells,
228 nature and origin of organic matrix, or a combination of these factors [1, 31, 32]. Different
229 types of cementum are formed at different rates, but only AEFC is considered annually

230 deposited. Most importantly, incremental lines are found in different types of cementum (e.g.
231 in acellular and cellular cementum). Furthermore, EDS analysis can only be used to obtain the
232 relative amounts of concretions even when certified standards are used; as EDS operating
233 software does not provide us with continuous elemental values. This might be the reason we
234 were not able to detect any obvious variation in Ca and P profiles. With all this in mind, we
235 argue that the SEM-EDS technique is inadequate for measuring the degree and distribution of
236 AEFC mineralization.

237 ToF-SIMS micro-image revealed clearly defined AEFC in our cross-section. Although some
238 appearance of layering within AEFC can be also observed (Fig 2a), the incremental lines of
239 AEFC were not clearly discernible from the micrograph. On the other hand, we were able to
240 estimate the approximate width of AEFC incremental lines using the micrograph itself. The
241 linescans showed obvious variation in Ca⁺ intensity across the AEFC width, but not for HAp⁺
242 (Fig 2b, Fig 3). Ca⁺ intensity variation has been detected in a form of a depletion which might
243 correlate with the with patient's pregnancies, as the depletion of Ca⁺ intensity corresponds to
244 the patient's 2nd – 5th life decade (Fig 3). The lowest point in Ca⁺ intensity depletion is recorded
245 at 32nd μm which corresponds to the beginning of the patient's 4th life decade. The initial Ca⁺
246 intensity depletion was detected four years prior to the patient's age at the time of the first
247 pregnancy. The lowest value of Ca intensity is measured around the age corresponding to the
248 patient's last pregnancy. From that point on, the intensity values for Ca⁺ are seen to rise or
249 perhaps normalise, after final pregnancy.

250 In conclusion, our ToF-SIMS results imply that life history parameters, such as pregnancies,
251 are more likely to influence AEFC in terms of relatively reduced mineralization, which is in
252 accordance with work done by Kagerer and Grupe [3]. We also demonstrated how use of SEM-
253 EDS technique is inadequate when measuring the degree and distribution of AEFC

254 mineralization. Our results point towards an alternative direction for life history research using
255 tooth cementum data. To detect life history parameters, which have a marked impact on Ca
256 metabolism, such as pregnancies, we propose a new methodological approach, namely Time-
257 of-Flight Secondary Ion Mass Spectrometry. As a clear relationship between degree and
258 distribution of AEFC mineralization and reported pregnancies is observed by our study, this
259 technique appears to have great potential for investigating various biological events in the
260 historical development of humans and animals. Clearly, more clinical tests are required. In the
261 meantime, far more caution is required by cementum-oriented life history researchers.

262

263 **Supporting Information**

264 **S1 Appendix. Transmitted Polarized Light Microscopy Analysis**

265 **S1 Table. Results of the reported counts of incremental lines from the tooth cross-**
266 **section.**

267 **S1 Fig. Ground cross-sections of the patient's tooth under the transmitted polarized light**
268 **microscope (a and b ×400).** The red arrows indicate a pronounced eruption line. The white
269 arrows indicate possible “crisis” lines which appear as broad and translucent layers in acellular
270 extrinsic fiber cementum (AEFC) of the patient. (D) represents dentine, and (CDJ) is cemento-
271 dentinal junction.

272

273 **References**

- 274 1. Berkovitz BG, Holland G, Moxham B. Oral Anatomy, Histology and Embryology. 4th
275 ed. Elsevier Limited; 2009.
- 276 2. Lieberman DE. Life history variables preserved in dental cementum microstructure.
277 Science. 1993; 261: 1162-1164. DOI: 10.1126/science.8356448.
- 278 3. Kagerer P, Grupe G. Age-at-death diagnosis and determination of life-history
279 parameters by incremental lines in human dental cementum as an identification aid.
280 Forensic Sci Int. 2001; 118: 75-82.
- 281 4. Kovacs CS, Kroneneberg HM. Maternal-fetal calcium and bone metabolism during
282 pregnancy, puerperium, and lactation. Endocrine Reviews. 1997; 18(6): 832-872.
- 283 5. Harada S, Rodan GA, Control of osteoblast function and regulation of bone mass.
284 Nature. 2003; 423: 349-355.
- 285 6. Cipriano A. Cold stress in captive great apes recorded in incremental lines of dental
286 cementum. Folia Primatol. 2002; 73: 21-31.
- 287 7. Cool SM, Forwood MR, Campbell P, Bennett MB. Comparisons between bone and
288 cementum compositions and the possible basis for their layered appearances. Bone.
289 2002; 30(2): 386-392.
- 290 8. Colard T, Falgayrac G, Bertrand B, Naji S, Devos O, Balsack C, et al. New Insights
291 on the Composition and the Structure of the Acellular Extrinsic Fiber Cementum by
292 Raman Analysis. PLoS ONE. 2016; 11(12): e0167316.
293 doi:10.1371/journal.pone.0167316
- 294 9. Laws RM. A new method of age determination for mammals. Nature. 1952: 972-973.
- 295 10. Stott GG, Sis RF, Levy BM. Cemental annulation as an age criterion in forensic
296 dentistry. J. Dent. Res. 1982; 61:814-7. PMID: 6953121
- 297 11. Lieberman DE, Meadow RH. The biology of cementum increments (with an
298 archaeological application). Mammal Rev. 1992; 22(2): 57-77.

- 299 12. Wittwer-Backofen U, Buba H. Age estimation by tooth cementum annulations. In:
300 Hoppa RD, Vaupel JW, editors. *Paleodemography: Age Distributions from Skeletal*
301 *Samples*. Cambridge: Cambridge University Press; 2002. pp. 107-128.
- 302 13. Bojarun R, Garmus A, Jankauskas R. Microstructure of dental cementum and
303 individual biological age estimation. *Medicina (Kaunas)*. 2003; 39(10): 960-4.
- 304 14. Wittwer-Backofen U, Gampe J, Vaupel JW. Tooth cementum annulation for age
305 estimation: Results from a large known-age validation study. *American Journal of*
306 *Physical Anthropology*. 2004; 123(2): 119-129.
- 307 15. Lippitsch A, Grupe G. Variability of the apposition of the acellular, extrinsic fiber
308 cementum and its influence on the tooth cementum annulation technique in humans:
309 the influence of physical demands and functional morphology. In: Grupe G, Peters J,
310 editors. *Skeletal Series and Their Socio-Economic Context*. Rahden/Westf. : M.
311 Leidorf; 2007. pp. 87-112.
- 312 16. Dias PE, Beaini TL, Melani RF. Age estimation from dental cementum incremental
313 lines and periodontal disease. *J. Forensic Odontostomatol*. 2010; 28: 13-21.
- 314 17. Kasetty S, Rammanohar M, Raju Ragavendra T. Dental cementum in age estimation:
315 a polarized light and stereomicroscopic study. *J. Forensic Sci*. 2010; 55: 779-783.
- 316 18. Radovic M. Ageing in the Danube Gorges population (9500 – 5500 BC) – Tooth
317 Cementum Annulation method. *Starinar*. 2012; 42: 9-18. doi:
318 10.2298/STA1262009R.
- 319 19. Schug GR, Brandt ET, Lukacs JR. Cementum annulations, age estimation, and
320 demographic dynamics in Mid-Holocene foragers of North India. *HOMO-Journal of*
321 *Comparative Human Biology*. 2012; 63(2): 94-109.

- 322 20. Gauthier J, Schutkowski H. Assessing the application of tooth cementum annulation
323 relative to macroscopic aging techniques in an archeological sample. *Homo*. 2013;
324 64:42-57. doi: 10.1016/j.jchb.2012.11.001 PMID: 23218650
- 325 21. Bertrand B, Robbins Schug G, Polet C, Naji S, Colard T. Age-at-death estimation of
326 pathological individuals: a complementary approach using teeth cementum
327 annulations *Int J Paleopathol*. 2016; 15:120-127. doi: 10.1016/j.ijpp.2014.04.001.
- 328 22. Lipsinic FE, Paunovich E, Houston GD, Robison SF. Correlation of age and
329 incremental lines in the cementum of human teeth. *J Forensic Sci*. 1986; 31(3):982-9.
- 330 23. Renz H, Radlanski RJ. Incremental Lines in Root Cementum of Human Teeth – A
331 Reliable Age Marker? *HOMO - Journal of Comparative Human Biology*. 2006; 57(1):
332 29-50. DOI:10.1016/j.jchb.2005.09.002
- 333 24. Naji S, Colard T, Blondiaux J, Bertrand B, d'Incau E, Bocquet-Appel J.
334 Cementochronology, to cut or not to cut? *International Journal of Paleopathology*.
335 2016; 15: 113-119. PMID: 29539545 DOI: 10.1016/j.ijpp.2014.05.003
- 336 25. Wittwer-Backofen U. Age Estimation Using Tooth Cementum Annulation. In: Bell
337 LS, editor. *Forensic Microscopy for Skeletal Tissues: Methods and Protocols*.
338 Totowa, NJ: Humana Press; 2012. p. 129-43.
- 339 26. Helm S, Seidler B. Timing of permanent tooth emergence in Danish children.
340 *Community Dentistry and Oral Epidemiology*. 1974; 2: 122-129. doi:10.1111/j.1600-
341 0528.1974.tb01669.x
- 342 27. Nelson SJ, Ash MM. *Wheeler's Dental Anatomy, Physiology, and Occlusion*. 9th ed.
343 St. Louis, Mo. : Saunders Elsevier; 2009.
- 344 28. Lieberman DE. The biological basis of seasonal increments in dental cementum and
345 their application to archaeological research. *J Archaeol Sci*. 1994; 21:525-539.

- 346 29. Hals E, Selvig KA. Correlated electron probe microanalysis and microradiography of
347 carious and normal dental cementum. *Caries Res.* 1997; 11:62-75.
- 348 30. Selvig KA, Hals E. Periodontally diseased cementum studied by correlated
349 microradiography, electron probe analysis and electron microscopy. *J Periodont Res.*
350 1977; 12:419-429. PMID: 145479
- 351 31. Yamamoto H, Niimi T, Yokota-Ohta R, Suzuki K, Sakae T, Kozawa Y. Diversity of
352 Acellular and Cellular Cementum Distribution in Human Permanent Teeth. *Journal of*
353 *Hard Tissue Biology.* 2009; 18(1): 40-44.
- 354 32. Ho SP, Marshall SJ, Ryder MI, Marshall GW. The tooth attachment mechanism
355 defined by structure, chemical composition and mechanical properties of collagen
356 fibers in the periodontium. *Biomaterials,* 2007; 28(35):5238-5245. doi:
357 10.1016/j.biomaterials.2007.08.031 PMID: 17870156

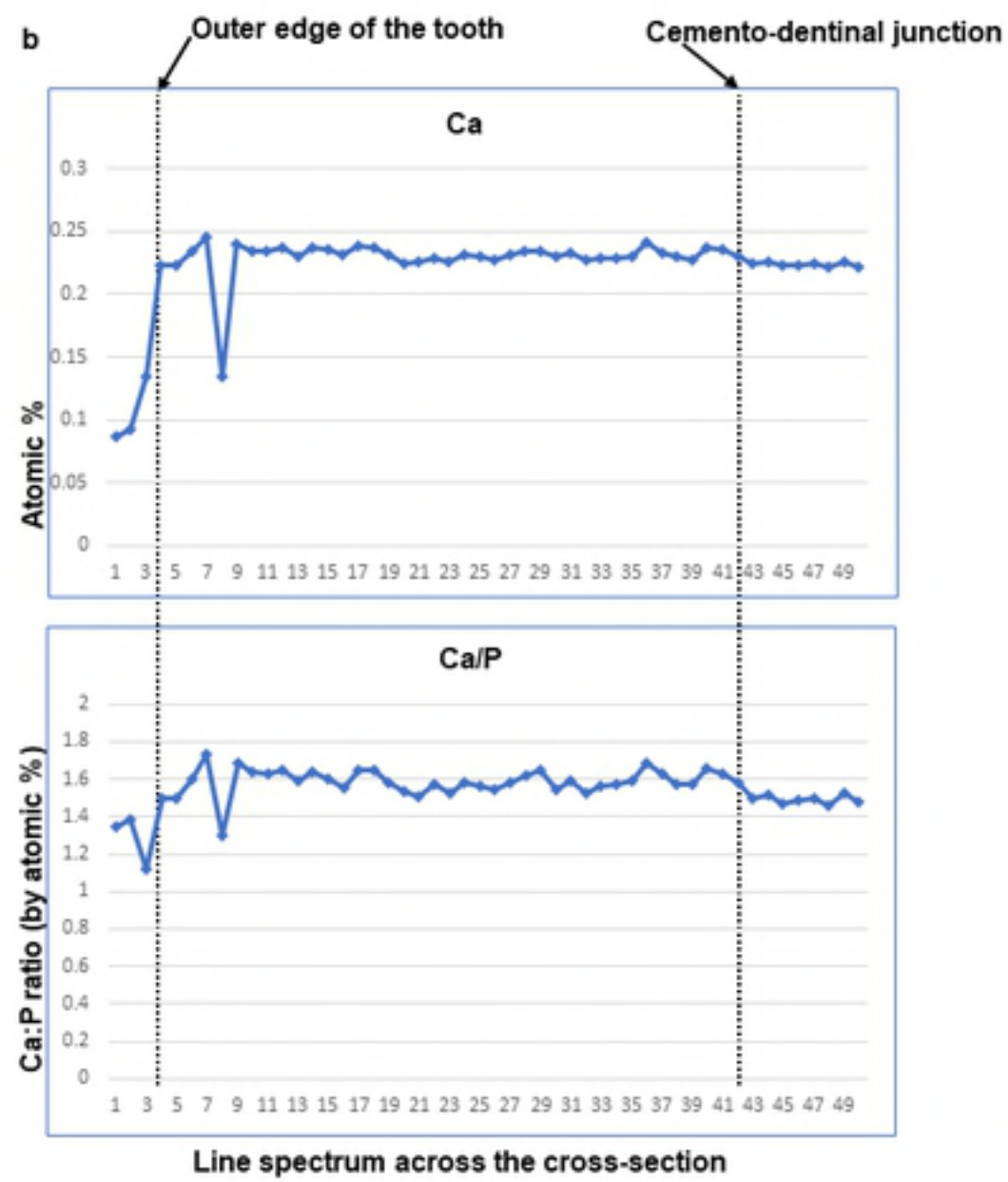
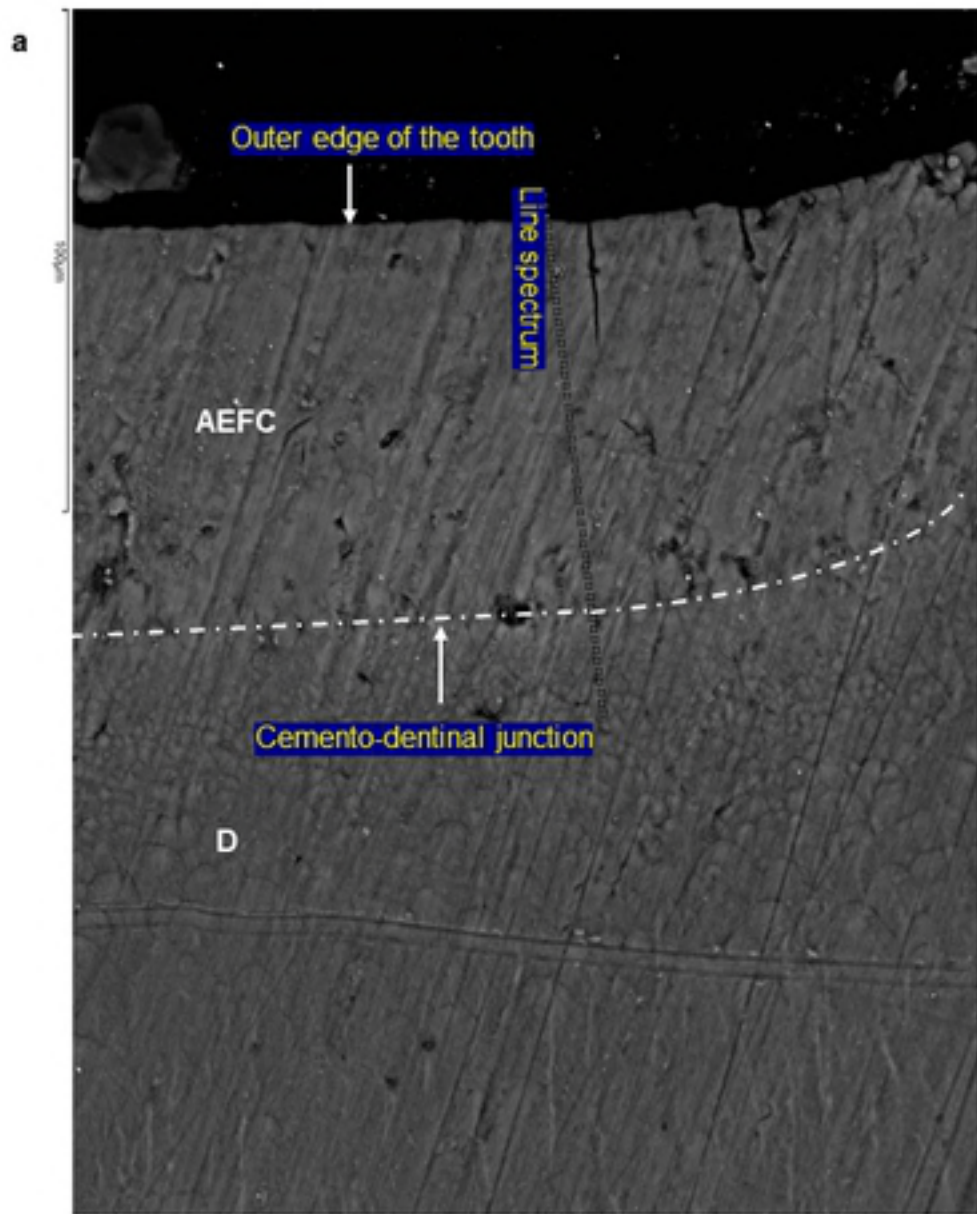


Figure 1

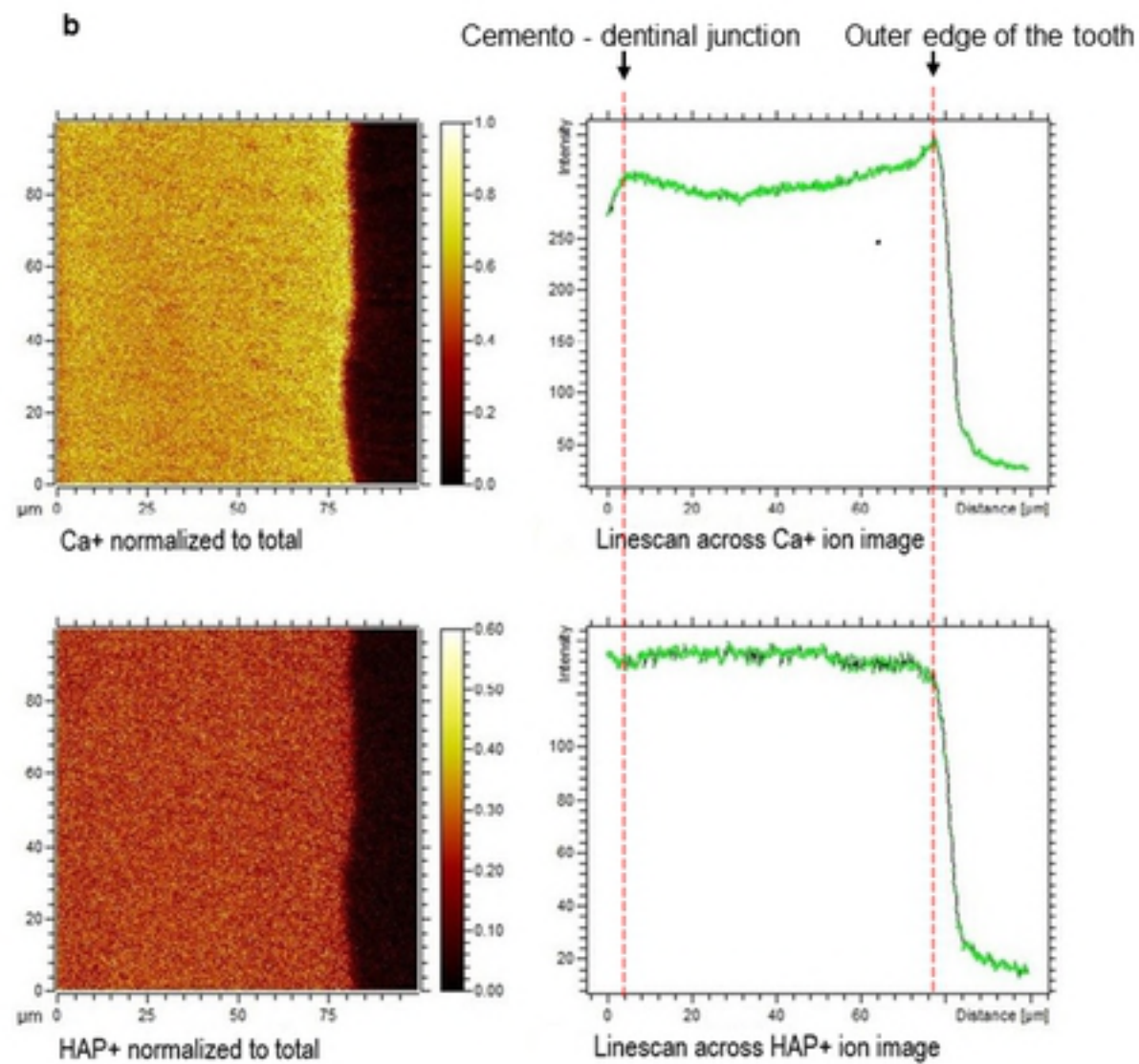
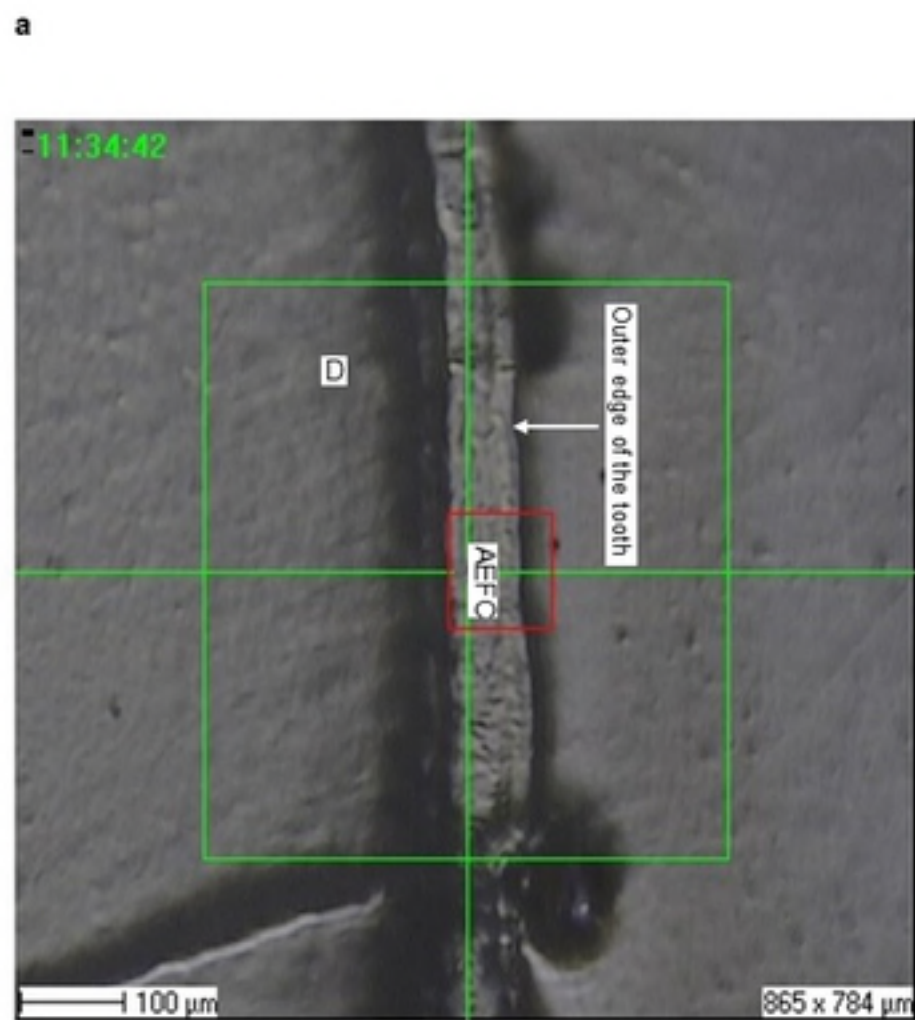


Figure 2

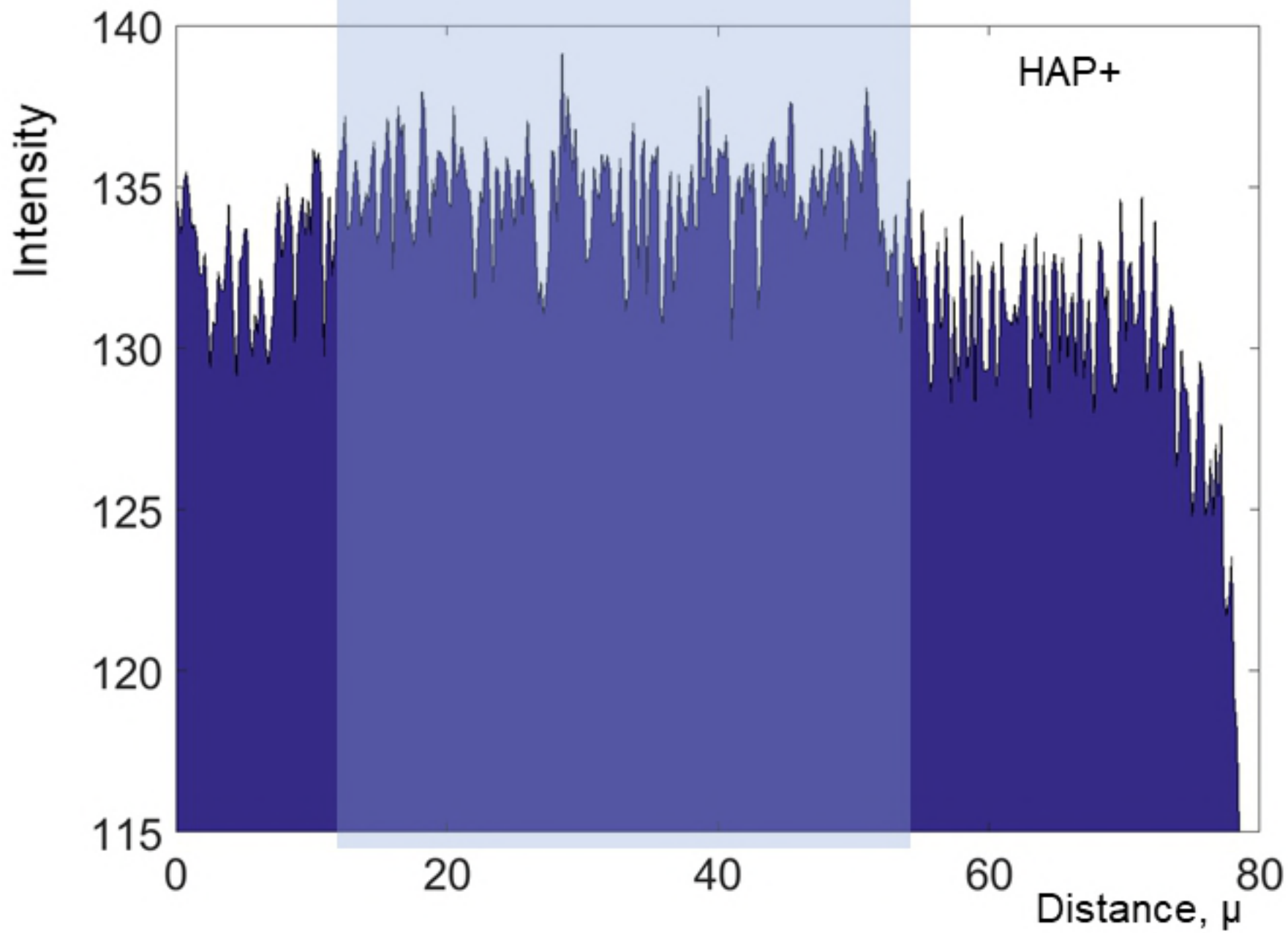
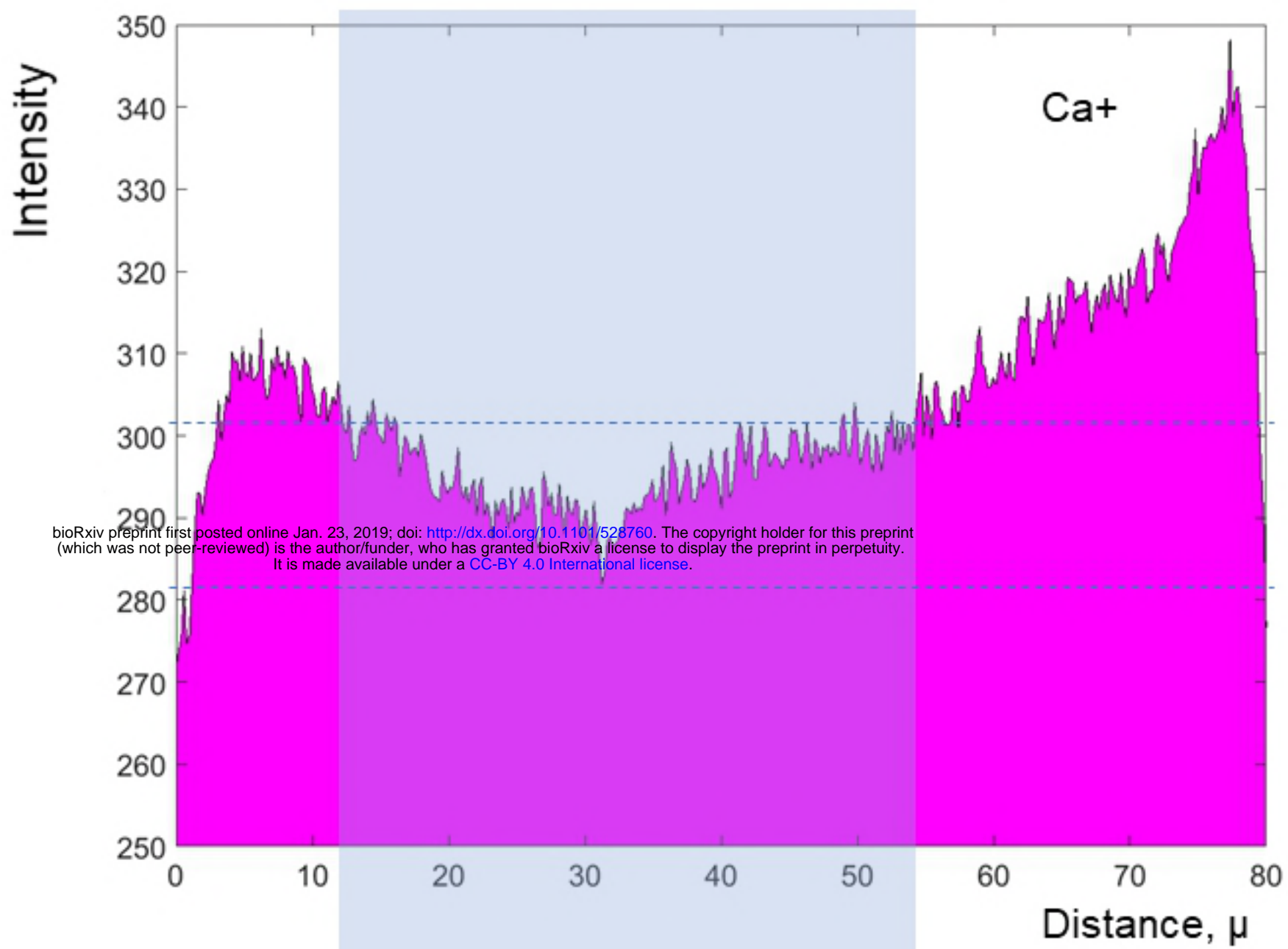


Figure 3